8th International Conference on CFD in Oil & Gas, Metallurgical and Process Industries
SINTEF/NTNU, Trondheim Norway *CFD11-147*
21-23 June 2011

INVESTIGATION OF TWO-PHASE SLUG FLOW IN A RISER USING PHYSICAL AND NUMERICAL SIMULATIONS

Mukhtar ABDULKADIR, Valente, HERNANDEZ-PEREZ, Ian S. LOWNDES* and Barry J. AZZOPARDI
Process and Environmental Engineering Research Division, Faculty of Engineering, University of Nottingham
University Park, Nottingham, NG7 2RD, United Kingdom

* E-mail: ian.lowndes@nottingham.ac.uk

ABSTRACT

Experimental investigations can prove to be expensive, risky and limited by the existing available techniques. In any industrial set-up time is always at premium and in an area where information is limited realistic and timely predictions are important. This paper presents the results of experimental and CFD studies of slug flow in a vertical riser using validated models.

An Electrical Capacitance Tomography (ECT) unit was used to monitor an air - silicone oil mixture flowing in a vertical 67 mm diameter riser. This enables the measurement of the instantaneous distribution of the flow phases over the cross - section of the pipe. The ECT sensor has two circumferential rings of electrodes, 89 mm apart (also known as twin - plane sensors) which enabled the determination of the rise velocity of any observed Taylor bubbles and liquid slugs.

The simulations were carried out using the commercial software package Star - CD and Star - CCM+, which is designed for numerical simulation of continuum mechanics problems. The model consisted of a cylindrical 67 mm internal diameter and 6 m vertical pipe. A butterfly mesh structure was employed in the computational domain. Air and silicone oil were used as the model fluids. The condition of two-phase slug flow was simulated with the Volume of Fluid (VOF) model, taking into consideration turbulence effects using the standard $k-\varepsilon$ model. The simulation predictions were validated both qualitatively and quantitatively against the experimental data and were then used to obtain further insights into the characteristics of slug flow.

A reasonably good agreement can be observed for the results of the experiment and computational fluid dynamics (CFD) based on the time series of void fraction. As was done for the experimental conditions, more information about the slug parameters for this particular case were obtained from the time series of void fraction, such as the dominant frequency, and therefore comparisons of the experimental results and CFD computations were also performed in terms of the Probability Density Function (PDF) of the time series and the Power Spectral Density (PSD). The study demonstrates the potential of Computational Fluid Dynamics (CFD) as a design tool.

Keywords: CFD, ECT, VOF, Slug flow, air - silicone oil, riser.

NOMENCLATURE

A	Area [m^2]
F	Frequency [Hz]
ε_g	Void fraction [-]
ε_{gs}	Void fraction in the liquid slug [-]
ε_{TB}	Void fraction in the Taylor bubble [-]
V_{TB}	Structure velocity [m/s]
L_{SU}	Length of the slug unit [m]
L_S	Length of the liquid slug [m]
L_{TB}	Taylor bubble length [m]
k	Kinetic energy of turbulence [m^2/s^2]
n	number of phases [-]
u	Velocity [m/s]
i, j	Space directions
q	Phase index

INTRODUCTION

The occurrence of slug flow in a vertical riser is a very common phenomenon under normal operating conditions of a two-phase flow facility, such as in an oil production riser. Considerable amount of research has been devoted to the study of this two-phase flow regime (Dumitrescu (1943); Moissis and Griffith (1962); Nicklin *et al.* (1962); White and Beardmore (1962); Brown (1965); Akagawa and Sekoguchi (1966); Wallis (1969); Collins *et al.* (1978); Fernandes *et al.* (1983); Mao and Dukler (1985); Mao and Dukler (1991); Barnea and Brauner (1993); DeJesus *et al.* (1995); Pinto and Campos (1996); Clarke and Issa (1997); van Hout *et al.* (2002); Taha and Cui (2006) among others. A critical review of this topic is given by Fabre and Line (1992). However, there remains much to investigate and understand of the flow pattern.

One of the features of the slug flow pattern is an acceleration of the liquid phase which results in the transition of fast liquid slugs, which carry a significant amount of liquid with high kinetic energy. It is potentially hazardous to the structure of the system due to the strong oscillating pressure levels produced from the liquid slug as well as the mechanical momentum of the slugs. It is therefore important to predict the flow behaviour. Empirical correlations and mechanistic models have been presented in the literature. These are one-dimensional approaches that cannot fully characterise the flow. The limitations of the one-dimensional models can be overcome using CFD. Successful applications of CFD in multiphase flow are highly dependent on the flow pattern under study, as different models are used for different flow patterns. As understood, multidimensional models in CFD must be generally able to capture the physics in all flow regimes. These models require to be validated in order to be applied confidently. CFD code validation requires experimental data that characterise the distributions of parameters within large flow domains.

In this work some slug flow parameters are determined using experiments and CFD.

EXPERIMENTAL METHODOLOGY

The experimental investigations were carried out on an inclinable pipe flow rig within the Chemical Engineering Laboratories of University of Nottingham. The details of the experimental facility can be found elsewhere, (e.g. Azzopardi et al (1997), Geraci et al. (2007a) and Geraci et al. (2007b), Hernandez-Perez et al (2008), and Abdulkadir et al. (2010)). In brief: the experimental test section of the facility consists of a transparent acrylic pipe of 6 m length and 0.067 m internal diameter. The test pipe section may be rotated on the rig to allow it to lie at any inclination angle of between -5 to 90^o to the horizontal. For the experiments reported in this paper the rig test pipe section was mounted as a vertical riser (an inclination of 90^o to the horizontal). It is worthy of mention that full-experimentation in risers of this magnitude and other larger ones is expensive and therefore a more cost-effective approach for exploring the behaviour of two-phase flow in these risers is by using validated CFD codes.

The resultant flow patterns created for the range of air - silicone oil injection circulation flow rates studied were recorded using electrical capacitance tomography (ECT). A detailed description of theory behind the ECT technology can be found elsewhere, for example, Hammer (1983), Huang (1995), Zhu *et al.* (2003) and Azzopardi *et al.* (2010). The use of two such circumferential rings of sensor electrodes, located at a specified distance apart (also known as twin - plane sensors), enabled the determination of the rise velocity of any observed Taylor bubbles and liquid slugs. The twin - plane ECT sensors were placed at a distance of 4.4 and 4.489 m upstream of the air - silicone oil mixer injection portal located at the base of the riser. A flow chart of the various experimental measurements recorded and the parameter calculations performed to characterise the observed slug flows are presented in Table 1. Parallel to the experiments, CFD calculations were carried out. The aim of the numerical simulations is the validation of prediction of the slug flow with the existing multiphase flow models, built in the commercial code Star-CD and Star-CCM+.

CFD MODEL

The commercial CFD software Star-CD and Star-CCM+ are used to simulate the motion of the Taylor bubbles rising in a flowing liquid through a vertical 67 mm internal diameter and 6 m height riser. In discretizing the computational domain, the Star-CD code uses the Finite Volume method.

Table 1: Table of Flowchart for experimental measurement used to obtain the parametric characterisation of the slug flow regime

Direct physical measurement		Data processing method	Parametric Output 1	Parametric Output 2
Instrument	Data			
ECT	Time series of void fraction	PDF of void fraction	Flow pattern, $\varepsilon_{gs}, \varepsilon_{TB}$, frequency	Lengths of liquid slug and Taylor bubble, symbols of parameter set
		PSD – Power Spectral Density	Frequency, symbols of parameter set	
		Cross-correlation	Structure velocity, symbol	
		Image reconstruction	Contours of phase distribution	3D structures

The movement of the gas-liquid interface is tracked based on the distribution of α_{G_1}, the volume fraction of gas in a computational cell, where $\alpha_G = 0$, in the liquid cell and $\alpha_G = 1$ in the gas phase, Hirt and Nichols (1981). Therefore, the gas - liquid interface exists in the cell where α_G lies between 0 and 1.

Computational domain

In order for the simulation to produce meaningful results, it was important to ensure that the geometry of the flow domain represented that of the experimental arrangement. Hence, a full 3-Dimensional domain, as shown in Figure 1, was considered based on the fact that the flow simulated has been found to be axisymmetric according to the experimental works of Azzopardi et al. (2010) and Hernandez-Perez et al. (2011). They employed conductance wire mesh sensor (WMS) to look at the flow distribution in a 67 mm internal diameter and 6 m vertical pipe (same as the one used in this study). They concluded that the classical Taylor bubble shape is rarely obtained when the pipe diameter is increased.

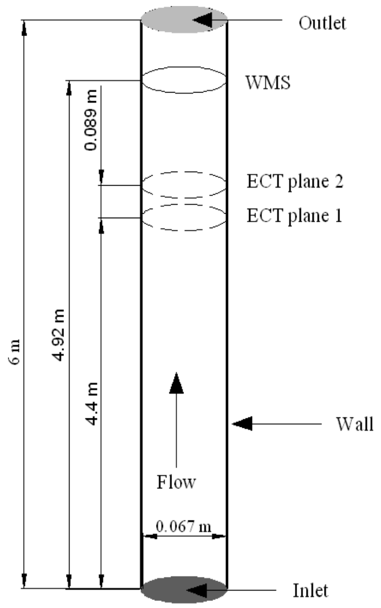

Figure 1: 3-D geometry of the computational domain showing the measurement locations and instrumentation.

In this work, two CFD measurement sections were placed at positions similar to those of the experimental work, namely, 4.4 m and 4.489 m, the two electrical capacitance tomography (ECT) planes. Air and silicone oil are supplied at the inlet section of the pipe, then the two - phase mixture flowed along the pipe, and is finally discharged through the outlet at atmospheric pressure. The relevant fluids properties are shown in Table 2.

Table 2: Properties of the fluids

Fluid	Density (kg/m^3)	Viscosity (kg/ms)	Surface tension (N/m)
Air	1.18	0.000018	
Silicone oil	900	0.0053	0.02

Gas – liquid mixing section

In the experimental set up, it was ensured that the mixing section of the air and silicone oil phases took place in such a way as to reduce flow instability. Flow stability was achieved by using a purpose built mixing device, providing maximum time for the two-phase to develop. The mixing device is made from PVC pipe as shown in Figure 2.The silicone oil enters the mixing chamber from one side and flows around a perforated cylinder. There, air is introduced through a large number of 3 mm diameter orifices. Thus, gas and liquid could be well mixed at the test section entry. Inlet volumetric flow rates of liquid and air are determined by a set of rotameters.

As for the CFD, at the inlet, a velocity-inlet boundary type is used in which the mixture velocity and the liquid volume fraction are specified. The velocity profile is assumed to be uniform. This approach requires no additional experimental knowledge about the slugs in order to set up the numerical simulation. This is also similar to the way the experimental work has been carried out.

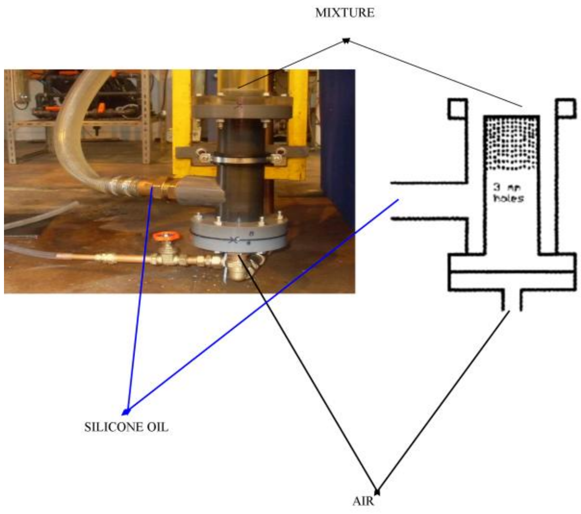

Figure 2: Gas liquid mixing section

Grid generation

It has been reported by Hernandez-Perez *et al.* (2011) and confirmed in this study that the mesh has a great influence on the solver convergence and solution of every CFD simulation. It is important to keep high mesh quality standards to ensure convergence and the accuracy of the simulation. The model geometry was built and meshed with Star-CD, then imported into Star-CCM+, where the computation and post-processing of the results were performed. The name of the mesh employed is known as butterfly grid. In this grid, a Cartesian mesh is used in the centre of the pipe combined with a cylindrical one around it. It requires multiple blocks but generally has the best grid quality in terms of orthogonality and mesh density. The construction of this mesh requires a more elaborated procedure, but it can be automated by implementing a macro in the Star-CD software. Details can be found in Hernandez-Perez *et al.* (2011).

The mesh density selected was based on the grid convergence study carried out in this work and Hernandez-Perez (2008), where a mesh with 500,000 cells for an inclined pipe of 6 m length and 38 mm diameter was found to be adequate for an inlet flow condition that consists of liquid and gas superficial velocities of 0.7 m/s and 1.6 m/s, respectively. However, in the present work, lower velocities are used.

Governing equations

The motion of an incompressible two-phase slug flow under isothermal conditions has been considered as the flow scenario in the present work. The Volume of Fluid (VOF) method, based on the Eulerian approach, implemented in the commercial CFD package Star-CCM+ is used in the numerical simulation. In addition, Star-CCM+ (2009) uses a High Resolution Interface Capturing Scheme (HRIC) based on the Compressive Interface Capturing Scheme for Arbitrary Meshes (CISCAM) introduced by Ubbink (1997) and enhanced by Muzaferija and Peric (1999). The body forces in the momentum equation consist of gravitational force and surface tension. Surface tension along an interface arises as a result of attractive forces between molecules in a fluid. In the VOF method, surface tension is introduced by adding a momentum source. The momentum equation, equation (2), is dependent on the volume fractions of all phases through the properties ρ and μ.

The mass, momentum and volume fraction conservation equations for the two-phase flow through the domain are represented as:

$$\frac{\partial \rho}{\partial t} + \frac{\partial \rho u_i}{\partial x_i} = 0 \qquad (1)$$

$$\frac{\partial \rho u_j}{\partial t} + \frac{\partial \rho u_i u_j}{\partial x_i} = -\frac{\partial P}{\partial x_j} + \frac{\partial}{\partial x_i}\mu\left(\frac{\partial u_i}{\partial x_j} + \frac{\partial u_j}{\partial x_i}\right) + \rho g_j + F_j$$

(2)

Where, P, g and F indicate, respectively, the pressure, the gravitational acceleration and the external force per unit volume. The momentum equation, shown above, is dependent on the volume fractions of all phases through the properties density (ρ) and viscosity (μ). For a two-phase flow system, if the phases are represented by the subscripts 1 and 2 and the volume fraction of the phase 2 is known, the ρ and μ in each cell are given by the following equation:

$$\rho = \alpha_2\rho_2 + (1-\alpha_2)\rho_1,\ \mu = \alpha_2\mu_2 + (1-\alpha_2)\mu_1 \qquad (3)$$

The interface between the two phases can be traced by solving the continuity equation for the volume fraction function:

$$\frac{\partial \alpha_q}{\partial t} + \frac{u_i \partial(\alpha_q)}{\partial x_i} = 0 \qquad (4)$$

Where u_i and x_i denote, respectively, the velocity component and the co-ordinate in the direction i (i =1, 2 or 3), t, being the time; and through the resolution of the momentum equation shared by the two considered fluids.

The primary-phase volume fraction will be computed based on the prevailing condition: the volume fraction equation for the primary phase in equation (4) will be obtained from the following equation:

$$\sum_{q=1}^{n} \alpha_q = 1 \qquad (5)$$

The continuum surface force (CSF) model proposed by Brackbill *et al.* (1991) was used to model the surface tension. With CSF model, the addition of surface tension to the VOF model calculation results in a source term in the momentum equation (2).

Solving these sets of equations has been done using a software package Star-CCM+. For the calculation of fluxes at control volume faces required by the VOF model, a second order discretization scheme was used, as recommended by the Star-CD (2009) code documentation.

Turbulence model

As the Taylor bubbles rises through the liquid, even in low flow rates, a developing film is created around the bubble and a wake at its tail. Therefore, turbulence must be considered in the numerical simulation. The accuracy of CFD solutions for turbulent flows can be affected by turbulence modelling, especially because of the complex features of the flow. According to Versteeg and Malalasekera (2007), it has been recognised by CFD users that, the choice of turbulence models used to represent the effect of turbulence in the time-averaged mean-flow equations represents one of the principal sources of uncertainty of CFD predictions. In order to simulate turbulence, the standard k-ε model, Launder and Spalding (1974), which requires that the flow is fully turbulent, was used for several reasons; the model is computationally-efficient, is implemented in many commercial codes, the pipe geometry is not complicated and it has demonstrated capability to simulate properly many industrial processes, including multiphase flow Ramos – Banderas *et al*. (2005), Cook and Behnia (2001) among others

Boundary and initial conditions

Once the mesh was generated, the boundaries of the computational domain were specified. All wall conditions were assumed to be no slip boundary. The no slip condition (v = 0) is the appropriate condition for the velocity component at solid walls. At the inlet, velocities for both phases were prescribed as superficial velocities: liquid 0.05 m/s and gas 0.34 m/s. The phases were clearly defined with the primary phase as oil and the secondary phase as air. The volume fraction and density of each phase were both prescribed at the inlet. The inlet values for turbulent kinetic energy, k, and its dissipation rate, ε, are estimated with the following equations proposed by Launder and Spalding (1974):

$$k_{in} = \frac{3}{2} I^2 U_{in}{}^2 \qquad (6)$$

$$\varepsilon_{in} = 2k_{in}{}^{3/2} / d \qquad (7)$$

$$I = \frac{0.16}{\mathrm{Re}^{1/8}} \qquad (8)$$

Where d is the pipe diameter, and I the turbulence intensity for fully developed pipe

Close to the wall, the standard wall function approach also based on the Launder and Spalding (1974) was employed to predict accurately the flow close to the walls. At the outlet, the remaining variables are transported out of the computational domain with zero average static pressure so that the mass balance is satisfied. Operating conditions were specified as being standard atmospheric pressure (101.3 kPa) and temperature 20^{o}C. Gravity effects are accounted for and the acceleration due to gravity to be -9.81 m/s^2 on the vertical.

Solution algorithm

In order to numerically solve the system of governing partial differential equations, discretisation of the equations has been carried out using a Finite Volume Method (FVM) with an algebraic segregated solver and co-located grid arrangement, as implemented in Star-CCM+(2009). In this grid arrangement, pressure and velocity are both stored at cell centres. Details of the discretisation (FVM) can be found elsewhere (e.g. Versteeg and Malalasekera (2007) and are hence omitted here. Since Star-CCM+ uses a segregated solver for VOF, the continuity and momentum equations need to be linked. Various techniques are reported in the literature. However, the SIMPLE algorithm, which stands for Semi-Implicit Method for Pressure-Linked Equations, Patankar and Spalding (1974), is applied to control the overall solution because of its good performance to find a fast converged solution. In addition, the iterative solver was speeded up tremendously by using an Algebraic Multigrid (AMG) technique to yield a better convergence rate.

All simulations in this work are performed under time dependent conditions. For the time dependent solution scheme, the main controlling factor is the time step. The time step was set to 2×10^{-4} seconds. This was became necessary in order to give a small number of time steps as possible whilst maintaining a smoothly converging solution. If a large time step is chosen, then the solution changes too much and is therefore likely to diverge. Inside each time interval iterations are carried out to resolve the transport equations for that time step. As long as the time step is small enough to get convergence, the smaller the time step, the fewer iterations, per time step are required. For this iteration process to converge, it may be necessary to control the change of the variables from one iteration to the next. This is achieved with under relaxation factors. Under relaxation factors of 0.3, 0.7 and 0.8 respectively were applied on pressure, momentum and turbulence kinetic energy parameters, as recommended by Star-CCM+ (2009).

An assessment of the degree to which the solution is converged can be obtained by plotting the residuals errors for each equation at the end of each time step. For a well-converged simulation, the maximum residual obtained was set to be around 10^{-4}; it is possible that a residual increases after any particular time step, but it does not necessarily imply that the solution is diverging. It is usual for residuals to occasionally get larger, such as at the beginning of a run.

Mesh independence study:

One of the most significant factors influencing the computation time is the size of the computational grid specified by the user. Mesh independence means that the converged solution obtained from a CFD calculation is independent of the grid density. In practice, mesh independence is indicated when further mesh refinement yields only small, insignificant changes in the numerical solution.

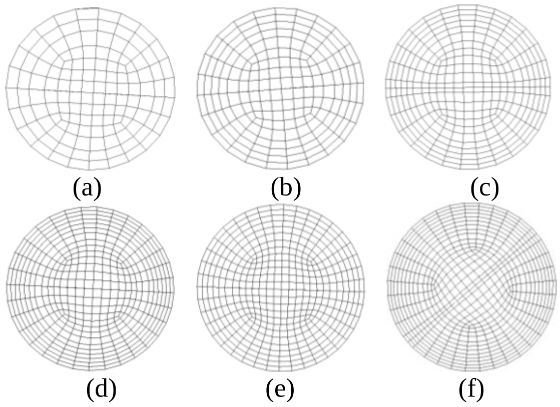

Figure 3: cross-sectional view of different sizes of computational grid used for mesh independent study (a) 26400 cells (b) 36000 cells (c) 54600 cells (d) 76800 cells (e) 84000 cells (f) 102600 cells

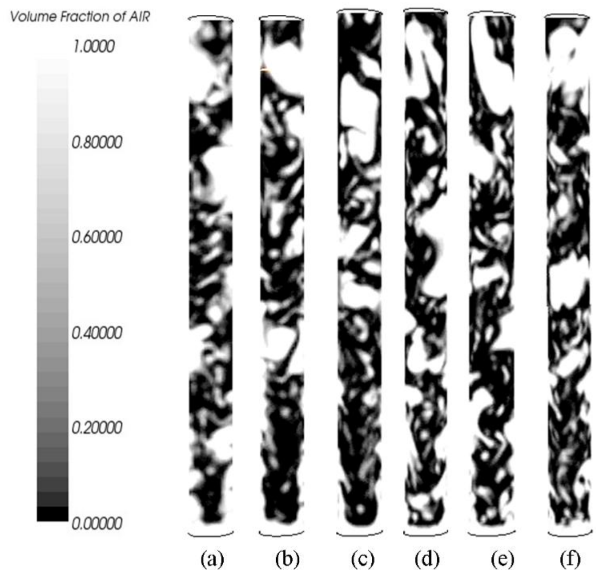

Figure 4: Contour plots of void fraction for different mesh densities (a) 26400 cells (b) 36000 cells (c) 54600 cells (d) 76800 cells (e) 84000 cells (f) 102600 cells

In order to identify the minimum mesh density to ensure that the solution is independent of the mesh resolution, a mesh sensitivity analysis has been carried out in the construction and analysis of the CFD model. In the mesh independence study, a computational domain of 1m length was used as this length is sufficient to carry out a test on the performance of the mesh with quite reasonably computational effort. Six 3-Dimensional meshes were investigated in the present study as shown in Figure 3 and the results of the study are presented in both Table 3 and Figure 4 for the general case of a vertical riser and a suitable grid resolution has been found.

Table 3: The results of obtained from the CFD mesh independence studies

<table>
<tr><th>Number of cells</th><th>Time series of void fraction</th><th>PDF of void fraction</th></tr>
<tr><td>26400</td><td>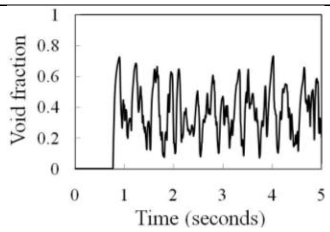</td><td>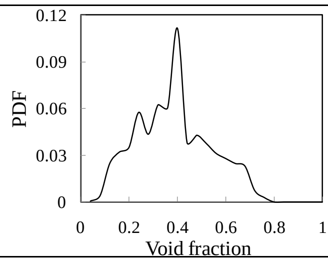</td></tr>
<tr><td>36000</td><td>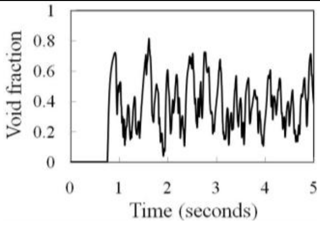</td><td>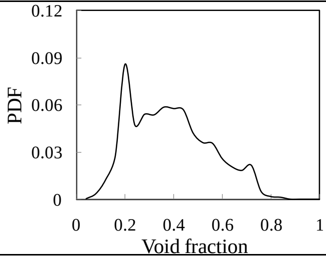</td></tr>
<tr><td>54600</td><td>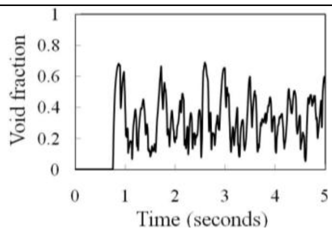</td><td>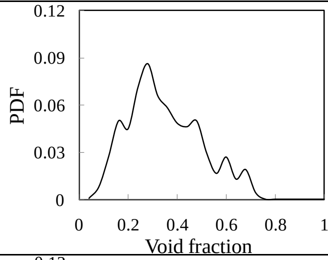</td></tr>
<tr><td>76800</td><td>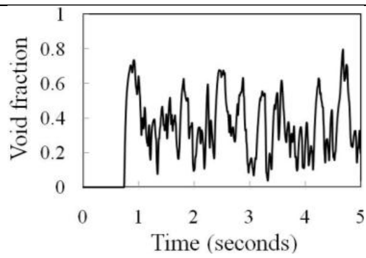</td><td>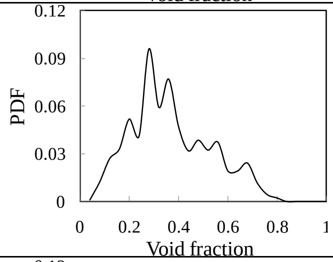</td></tr>
<tr><td>84000</td><td>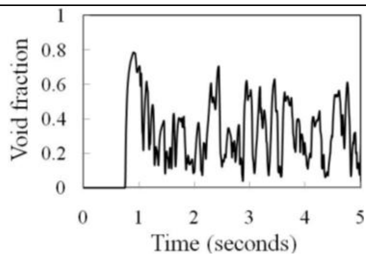</td><td>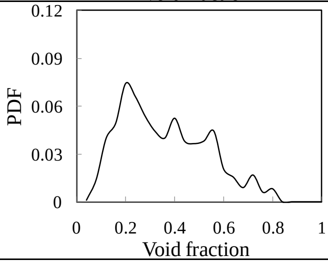</td></tr>
<tr><td>102600</td><td>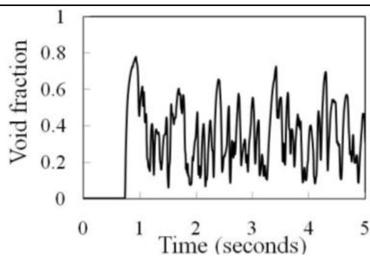</td><td>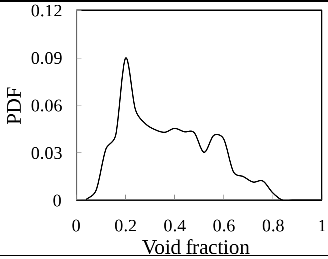</td></tr>
</table>

An insight into the effect of mesh density can be obtained from the contours of phase distribution in a longitudinal sectional view at the centre of the pipe, at a time when the flow, injected as a homogeneous two-phase mixture with a uniform velocity profile, has travelled from the inlet to the outlet section, Figure 3. This shows that bubbles are formed as the flow moves upwards, with a sharper gas - liquid interface as the mesh density is increased. However, no clear difference in terms of the flow pattern can be established.

In order to quantify the effect of the mesh density, the time series of cross sectional average void fraction has been recorded at a plane located at 0.5 m from the inlet for a time interval of 5 seconds. Results are presented in Table 3. In order to determine the time series of void fraction, the following procedure similar to that used by Hernandez - Perez (2008) was performed: a cross-sectional plane is defined at the measurement location, and the Area-Weighted Average value of the void fraction is calculated. The cross-sectional average void fraction is computed by dividing the summation of the product of the air volume fraction and facet area by the total area of the surface as follows:

$$\frac{1}{A}\int \varepsilon A = \frac{1}{A}\sum_{i=1}^{n}\varepsilon |A_i| \quad (9)$$

What we can see from Table 3 is that the times that it takes for the leading Taylor bubbles to arrive to the measuring section are: 0.692, 0.679, 0.651, 0.625, 0.624, and 0.625 seconds for the six meshes in order of increasing mesh density. The differences between these arrival times are small, in particular between the two bigger mesh densities (0.16 %). As the time increases and the intermittent flow pass though the measuring section, it became difficult to compare the time series directly. In view of this development, we decided to use statistical tools, Probability density function (PDF). In this case the graphs of probability density function (PDF) have been obtained and it can be observed that they vary with mesh density for all cases.

It is concluded that the PDFs of the predicted void fractions for the 84000 and 102600 cells are quite similar. For the range of mesh sizes studied, the void fraction was observed to fluctuate over the range, 0.05 and 0.8, whilst the minimum and maximum peak PDF are given by 0.074 and 0.117, respectively. However, for the PDF of void fraction for the 84000 and 102600 cells, the void fraction is the same, 0.2 whilst the height of the peak of the PDF are 0.074 and 0.09 for the 102600 and 84000 cells, respectively. Therefore, it can be concluded that the mesh with 84000 cells is adequate, as the change in the results produced is very small when the number of cells is increased to 102600, and it requires less computational effort than the one of 102600. Since the simulation involves a 6 m pipe, we decided to multiply the selected mesh size, 84000 cells by 6 to produce approximately 500,000 cells.

RESULTS AND DISCUSSION

The comparison between the results obtained from the CFD and experiment will be based on time series of void fraction, probability density function (PDF) of void fraction and power spectral density (PSD) of void fraction. A stop watch will be used to verify the time that it took the first bubble to arrive at the measurement section. This will be carried out at same liquid and gas superficial velocities of 0.05 and 0.34 m/s, respectively.The model fluid is air-silicone oil.

Comparison between the Computational fluid dynamics (CFD) and experiment

The PDF of void fraction both for the CFD and experiment predict the same flow pattern as slug flow, according to the definition of Costigan and Whalley (1996). According to them, slug flow is a flow pattern characterised by a PDF graph with two peaks, one at lower void fraction (liquid slug) and the other one at higher void fraction, Taylor bubble.

From Figure 5, it is interesting to observe that the CFD simulation is able to mimic the appearance of the first Taylor bubble (leading) as observed from the experiment. From the plot of the time series of void fraction for the CFD, the Taylor bubble first got to the measurement location from the mixing section in about 5.1 seconds whilst for the experiment, 5.7 s. A time interval of 5.2 seconds was recorded using a stop watch. The % time delay is 1.9 and 9.6 for the CFD and experiment, respectively. The % delay can be attributed to the uncertainty in taking measurements of the time the Taylor bubble departs the mixing section and reached the measurement location.

The contours of phase distribution as shown in Figure 6 (a) - (b) and Figure 7 (a) - (b) for the Taylor bubble obtained from both the CFD and experiment show a reasonably good agreement. It is worth mentioning that the CFD as shown in Figure 8 (a) - (b) is able to replicate what is happening at the tail of the Taylor bubble (wake), a feat that cannot be achieved with the experiment. Three regions can be observed from the velocity profiles in Figure 8(a) - (b): the Taylor bubble, falling film and the wake region. From the plot, the Taylor bubble can be seen moving vertically upwards whilst the liquid film on the other hand, downwards due to the action of gravity and the shape of the nose of the Taylor bubble. A similar observation was reported by Mao and Dukler (1991), van Hout et al. (2002) and Legius *et al.* (1995) who all worked on vertical pipes using air and water as the model fluid. The falling film with some entrained bubbles drop into the wake region and a vortex region is created. The liquid film and some of the entrained bubbles are subsequently carried upwards by the incoming gas phase. This behaviour is similar to that observed by Fernandes et al. (1983) and Shemer *et al*. (2004) that the rising bubbles in the liquid slug rise from entrainment of gas from the Taylor bubble base.

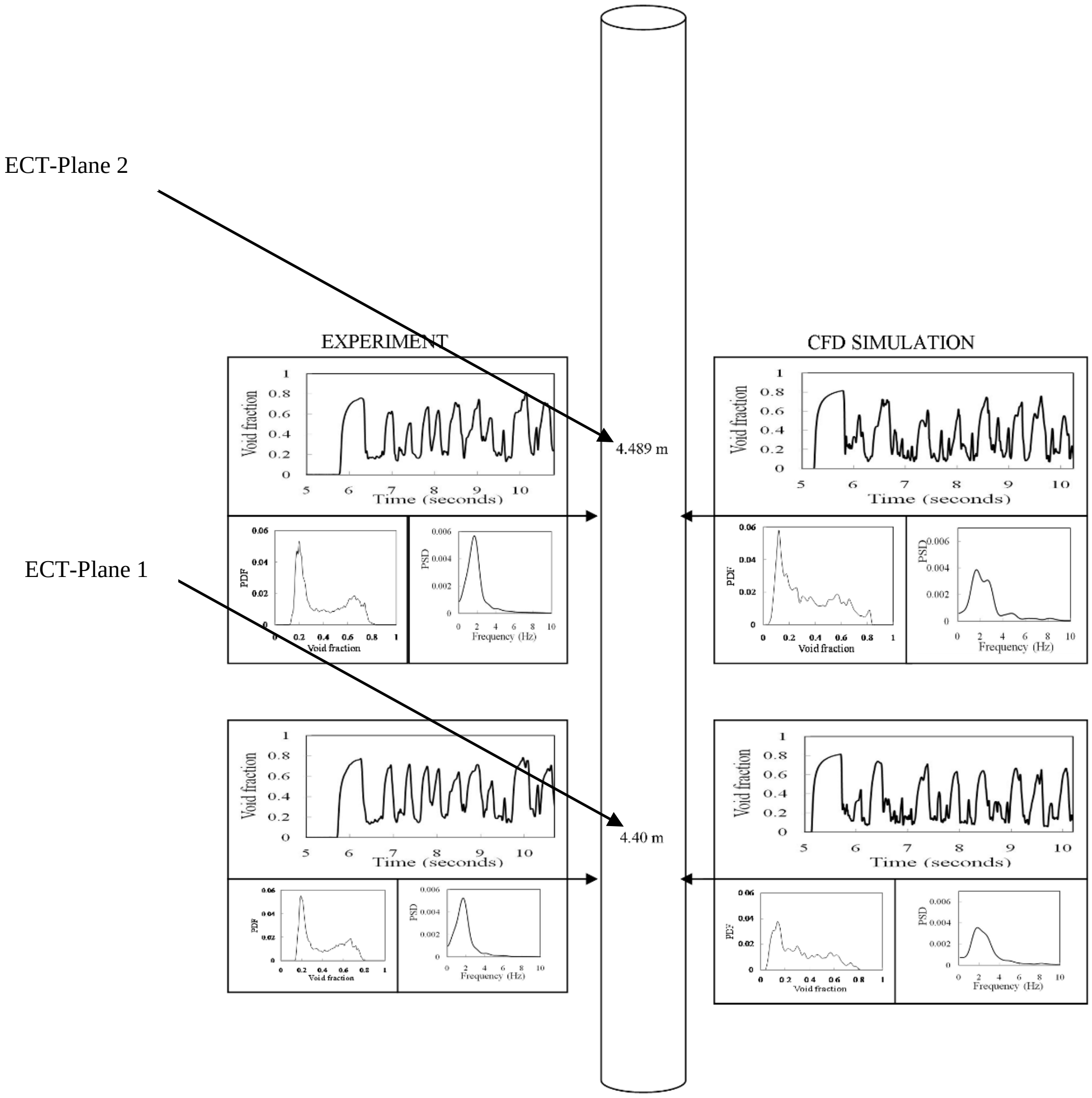

Figure 5: Comparison between experimental data and CFD simulation results (same method of introducing the liquid into the flow domain)

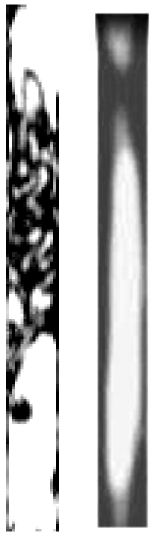

(a) (b)

Figure 6: comparison of contours of phase distribution, same inlet velocity condition for (a) CFD (b) ECT. The liquid and gas phases are represented by dark and light colours, respectively

Much of this entrained gas is swept around a vortex in the Taylor bubble wake and re-enters the bubble. This agreement suggest that the CFD simulation can be considered to be useful for obtaining other flow parameters that characterize the internal structure of the flow that are difficult to measure experimentally, such as the velocity field and phase distribution.

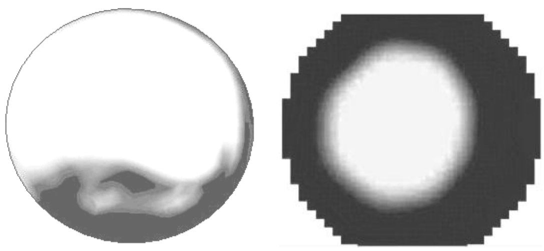

(a) (b)

Figure 7: Contours of phase distribution (cross-sectional void fraction of air) for the Taylor bubble obtained from (a) CFD (b) ECT. Screen shots taken at liquid and gas superficial velocity of 0.05 and 0.34 m/s, respectively.

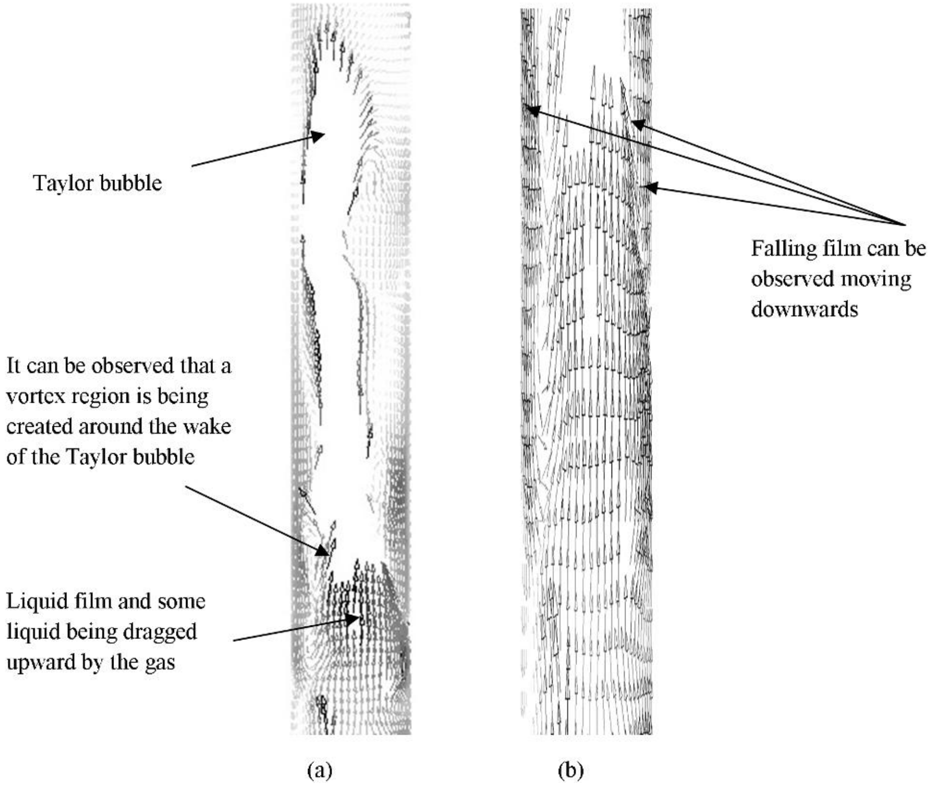

Figure 8: velocity profile around the (a) Taylor bubble (b) Wake region of the Taylor bubble for liquid and gas superficial velocity of 0.05 and 0.34 m/s, respectively obtained from CFD

The experiment was carried out with the pipe first full of liquid, before injecting air (gas), as was done for the CFD. This was done to give us confidence in our results; by comparing like with like.

CONCLUSION

A comparison between the results obtained from the CFD simulation and experiments has been carried out and the following conclusions can be drawn:

1) This work also confirms the results reported in the literature for the characteristics of slug flow.
2) A reasonably good agreement was obtained, and the CFD simulation can be used to characterize the slug flow parameters with confidence. However, further parametric CFD studies might be required to close the gap between CFD simulations and the experimental results.

ACKNOWLEDGEMENTS

M. Abdulkadir would like to express sincere appreciation to the Nigerian government through the Petroleum Technology Development Fund (PTDF) for providing the funding for his doctoral studies.
This work has been undertaken within the Joint Project on Transient Multiphase Flows and Flow Assurance. The Authors wish to acknowledge the contributions made to this project by the UK Engineering and Physical Sciences Research Council (EPSRC) and the following: - Advantica; BP Exploration; CD-adapco; Chevron; ConocoPhillips; ENI; ExxonMobil; FEESA; IFP; Institutt for Energiteknikk; Norsk Hydro; PDVSA (INTERVEP); Petrobras; PETRONAS; Scandpower PT; Shell; SINTEF; Statoil and TOTAL. The Authors wish to express their sincere gratitude for this support.

REFERENCES

ABDULKADIR, M., HERNANDEZ-PEREZ, V., SHARAF, S., LOWNDES, I. S. & AZZOPARDI, B. J., (2010). Experimental investigation of phase distributions of an air-silicone oil flow in a vertical pipe. World Academy of Science, Engineering and Technology (WASET), 61, 2010, 52-59

AZZOPARDI, B. J., (1997). Drops in annular two-phase flow. International Journal of Multiphase Flow 23, S1-S53.

AZZOPARDI, B. J., ABDULKAREEM, L.A., SHARAF, S., ABDULKADIR, M., HERNANDEZ-PEREZ, V., & IJIOMA, A., (2010). Using tomography to interrogate gas-liquid flow. In: 28th UIT Heat Transfer Congress, Brescia, Italy, 21-23 June.

AKAGAWA, K., & SAKAGUCHI, T., (1966). Fluctuation of void fraction in gas-liquid two-phase flow. Bulletin JSME, 9, 104-110

BARNEA, D., & BRAUNER, N., (1993). A model for slug length distribution in gas-liquid slug flow. International Journal of Multiphase Flow, 19, 829-838

BRACKBILL, J.U., KOTHE, D.B., & ZEMACH, C. (1992). A continuum method for modelling surface tension, Journal of Computational Physics, 100, 335-354.

BROWN, R. A. S., (1965). The mechanics of large gas bubbles in tubes: I. Bubble velocities in stagnant liquids. Canadian Journal of Chemical Engineering, 43, 217-223

BUGG, J.D., MACK, K. & REZKALLAH, K.S., (1998). A numerical model of Taylor bubbles rising through stagnant liquid in vertical tubes. International Journal of Multiphase Flow, 24, 271–281.

CLARKE, A. & ISSA, R. I., (1997), A numerical model of slug flow in vertical tubes. *Computers and Fluids*, 26, 4, 395-415.

COLLINS, R., DE MORAES, F. F., DAVIDSON, J. F., & HARRISON, D., (1978), The motion of a large gas bubble rising through liquid flowing in a tube. *Journal of Fluid Mechanics*, 89, 497-514.

COOK, M. & BEHNIA, M., (2001), Bubble motion during inclined intermittent flow. International Journal of Multiphase Flow, 22, 543 - 551.

COSTIGAN, G., & WHALLEY, P. B., (1996), Slug flow regime identification from dynamic void fraction measurements in vertical air-water flows. *International Journal of Multiphase Flow*, 23, 263-282

DAVIES, R.M. & TAYLOR, G.I., (1950), The mechanics of large bubbles rising through extended liquids and through liquids in tubes. *Proceedings of the Royal Society*, A 200, 375-395

DEJESUS, J.D., AHMAD, W., & KAWAJI, M., (1995), Experimental study of flow structure in vertical slug flow. *Advances in Multiphase Flow*, 31, 105-118

DUMITRESCU, D. T. (1943), Stromung an einer luftblase in senkrechten rohr Z angrew *Math Mech*, 23, 139-149

FABRE, J., & LINE, A., (1992), Modelling of two-phase slug flow. *Annual Review of Fluid Mechanics*, 24, 21-46

FERNANDES, R. C., SEMIAT, R., & DUKLER, A.E., (1983), Hydrodynamics model for gas-liquid slug flow in vertical tubes. *AIChE Journal*, 29, 981-989

GERACI, G., AZZOPARDI, B. J., & VAN MAANEN, H. R. E., (2007a), Inclination effects on circumferential film distribution in annular gas/ liquid flows, *AIChE Journal*, 53, 5, 1144-1150.

GERACI, G., AZZOPARDI, B. J., & VAN MAANEN, H .R .E. (2007b), Effects of inclination on circumferential film thickness variation in annular gas/ liquid flows. *Chemical Engineering Science*, 62, 11, 3032-3042.

HERNANDEZ-PEREZ, V., (2008), Gas-liquid two-phase flow in inclined pipes. *PhD thesis*, University of Nottingham.

HERNANDEZ-PEREZ, V., ABDULKADIR, M., & AZZOPARDI, B. J., (2011), Grid generation issues in the CFD modelling of two-phase flow in a pipe. *The Journal of Computational Multiphase Flow,3,13-26*

HAMMER, E. A., (1983),Three –component flow measurement in oil/ gas/ water mixtures using capacitance transducers. *PhD thesis*, University of Manchester

HIRT, C. W. & NICHOLS, B. D., (1981), Volume of Fluid (VOF) Method for the Dynamics of Free Boundaries, *Journal of Computational Physics*, 39, 201.

HUANG, S. M., (1995), Impedance sensors-dielectric systems. In R. A. Williams, and M. S. Beck (Eds.). *Process Tomography*, Cornwall: Butterworth-Heinemann Ltd.

LAUNDER, B. & SPALDING, D., (1974), The numerical computation of turbulent flows, *Computer Methods in Applied Mechanics and Engineering*, 3, 269-289.

LEGIUS, H.J.W.M., NARUMO, T.J. & VAN DEN AKKER, H.E.A., (1995), Measurements on wave propagation and bubble and slug velocities in concurrent upward two-phase flow. *Two Phase Flow Modelling and Experimentation*, Editizioni ETS, 907-914

MAO, Z. S., & DUKLER, A.E., (1985), Brief communication: Rise velocity of a Taylor bubble in a train of such bubbles in a flowing liquid. *Chemical Engineering Science*, 40, 2158-2160

MAO, Z. S. & DUKLER, A. E., (1991), The motion of Taylor bubbles in vertical tubes. II. Experimental data and simulations for laminar and turbulent flow, *Chemical Engineering Science*, 46, 2055-2064.

MAO, Z. S. & DUKLER, A. E., (1990), The motion of Taylor bubbles in vertical tubes. I. A numerical investigation for the shape and rise velocity of Taylor bubbles in stagnant and flowing liquid, *Journal of computational physics*, 91, 132-160.

MOISSIS, R., & GRIFFITH, P., (1962), Entrance effects in two-phase slug flow. *ASME Journal of Heat Transfer*, 366-370

MUZAFERIJA, S. & PERIC, M., (1999), Computation of free surface flows using interface-tracking and interface-capturing methods, Chap.2 in O. Mahrenholtz and M. Markiewicz (eds.), Nonlinear Water Wave Interaction, *Computational Mechanics Publication*, WIT Press, Southampton

NICKLIN, D. J., WILKES, J. O., & DAVIDSON, J. F., (1962), Two-phase flow in vertical tubes. *Transaction of Institution of Chemical Engineers*, 40, 61-68

PATANKAR, S.V. & SPALDING, D.B., (1972), A calculation procedure for heat, mass and momentum transfer in three dimensional parabolic flows", *Int. J. of Heat and Mass Transfer*, 15, 1787.

PINTO, A. M. F. R. & CAMPOS, J. B. L. M., (1996), Coalescence of two gas slugs rising in a vertical column of liquid, *Chemical Engineering Science*, 51, 45-54

RAMOS – BANDERAS, A., MORALES, R.D., SANCHEZ – PEREZ, R., GARCIA – DEMEDICES, L. & SOLORIO – DIAZ, G, (2005), Dynamics of two – phase downwards flow in submerged entry nozzles and its influence on the two – phase flow in the mold. International Journal of Multiphase flow, 31, 643-665.

SHEMER, L., GULITSKI, A., & BARNEA, D., (2004), Velocity field in the Taylor bubble wake measurements in pipes of various diameters, *24nd European Two-phase Flow Group Meeting*, Geneva

STAR-CD Version 4.10 & STAR-CCM+ Documentation, (2009), CD-adapco

TAHA, T., & CUI, Z.F., (2006). CFD modelling of slug flow in vertical tubes. *Chemical engineering science*, 61, 676-687

UBBINK, O., (1997), Numerical prediction of two fluid systems with sharp interfaces, *PhD thesis*, University of London

VAN HOUST, R., BARNEA, D., & SHEMER, L., (2002), Translational velocities of elongated bubbles in continuous slug flow. *International Journal of Multiphase flow*, 28, 1333-1350.

VERSTEEG, H.K. & MALALASEKERA, W., (2007), An Introduction to Computational Fluid Dynamics: the Finite Volume Method. 2nd ed. Pearson Educational Limited.

WALLIS, G. R., (1969), One- dimensional two-phase flow. McGraw-Hill, New York

WHITE, E. T. & BEARDMORE, R. H., (1962), The velocity of rise of single cylindrical air bubbles through liquids contained in vertical tubes. *Chemical Engineering Science*, 17, 351-361.

ZHU, K., MADHUSUDANA RAO, S., WANG, C., & SUNDARESAN, S., (2003), Electrical capacitance tomography measurements on vertical and inclined pneumatic conveying of granular solids. *Chemical Engineering Science*, 58, 4225-4245